

QUANTUM PHOTONICS

https://doi.org/10.1070/QEL17573

Principle of measuring the electron population of a quantum dot using a single-photon transistor based on an array of quantum dots

A.V. Tsukanov

Abstract. **The scheme of a single-photon transistor formed by an array of semiconductor single-electron quantum dots in an optical resonator is considered. The spectral response of such a transistor depends on the Coulomb interaction of the electrons of the array with the electron at the measured quantum dot. An approximate analytical expression is obtained for the response function of a transistor with an arbitrary number of quantum dots. Using a one-dimensional array (chain) as an example, the dependences of the transistor response on the chain period, on the distance to the measured quantum dot, and on the degree of compensation for Coulomb effects are analysed. It is shown that the electron–photon dynamics of the transistor is substantially affected by the Förster effect, the suppression of which by alternating quantum dots with different symmetry of the excited state significantly increases the measurement accuracy.**

Keywords: *quantum measurement, electrons, photons, microcavities, quantum dots, Coulomb interaction.*

1. Introduction

Detection of individual electrons and determination of their spatial position is an important practical problem. Its complexity is associated with the small value of the elementary charge, as well as with its high mobility in the crystal. Nevertheless, electrons can be localised inside the semiconductor matrix in small volumes, the band structure of which differs from the structure of the rest of the crystal due to the presence of an impurity. Such regions, which arise naturally in the form of nanocrystallites in gallium arsenide (GaAs) and silicon germanium (SiGe) solid solutions as a result of the Stranski–Krastanov phase transition, or are created using external electric fields, are called quantum dots (QDs) [1–3]. Electrons with the energy less than the jump in the energy of the conduction band bottom at the boundary between the QD and the crystal cannot leave the QD without giving them additional energy to compensate for this difference. Thus, an ordered QD nanostructure is created with a controlled number of electrons, the position of which in space is determined with an error specified by the QD size.

One-electron devices are widely used in micro- and nanoelectronics, being, in essence, the last generation of devices, the principles of which find a satisfactory description within the framework of the classical theory [4, 5]. Their further miniaturisation turns out to be impossible due to the indivisibility of the elementary charge. In addition, with a decrease in the characteristic size of QDs to values of the order of the de Broglie wavelength, quantum effects begin to play a decisive role in the dynamics of electrons. These effects can be used as the basis for a new class of devices that operate in accordance with the laws of the quantum world. Such devices, prototypes of which already exist and are being tested, include quantum bits (qubits), where the electronic states of QDs are used as logical states [6–10]. Other devices of a new type are highly sensitive electric field sensors – a single-electron transistor (SET) [11] and a quantum point contact [5, 12], inside which a nanoampere current flows, which responds to changes in the external field. The evolution of their state is correctly described by the equations of quantum mechanics. In most QD-based quantum computing schemes, qubits and sensors are combined into a structure sometimes called a quantum chip [13]. As is known, reliable measurement of the state of a qubit is necessary for the successful execution of any quantum algorithm [14]. An electron in different logical states of a QD qubit has different effects on the current state of the sensor. This makes it possible to determine the state of a qubit by the magnitude of the current through the adjacent SET.

Possessing a number of unique characteristics, capacitive electric field sensors also have several significant disadvantages. Significant difficulties are associated with the fabrication of the structure itself, which consists of more than ten metal electrodes with individual control and complex geometry. An equally serious problem is the undesirable interaction of the current not only with the measured qubit, but also with neighbouring ones. As an alternative version of the measuring device, we proposed a model of a single-photon transistor (SPT), in which the QD qubit itself plays the role of a sensitive element that affects the throughput of the photonic mode of the waveguide [15]. In this case, SPT photons (in contrast to SET electrons) interact in the near-field mode only with the measured qubit. However, the spatial separation of the photonic (measuring) and electronic (logical) subsystems turns out to be impossible here because of the rapid decrease in the energy of their interaction with the distance between them. In addition, even when the qubit is placed at the antinode of the photonic mode, this energy is quite small and comparable with the value of the uncontrolled spread of QD frequencies and with the rates of dissipative processes, which reduces the efficiency of qubit measurement.

In the present paper, we consider a scheme in which an increase in the SPT sensitivity is achieved by using not one QD, but an ordered array of QDs as a sensor element [16–21].

A.V. Tsukanov Valiev Institute of Physics and Technology, Russian Academy of Sciences, Nakhimovskii prosp. 34, 117218 Moscow, Russia; e-mail: a-v-ts@mail.ru

Received 24 April 2021; revision received 1 June 2021
Kvantovaya Elektronika **51** (8) 718–726 (2021)
Translated by V.L. Derbov

The measured QD qubit is located outside the device and electrostatically interacts with the electrons of the array of QDs located at the antinodes of the single-photon field of a waveguide or microcavity (MC). This interaction causes Coulomb shifts of the transition frequencies in each of the QDs of the array, which, in turn, affect the efficiency of the electron-photon coupling between the QD array and the mode. Thus, the presence or absence of an electron in the measured QD indirectly regulates the coefficient of transmission of photons through the SPT. Using the exponential-power model for the QD potential, we calculated both diagonal and off-diagonal matrix elements of the Coulomb interaction of electrons in two arbitrary QDs. In the subphoton field approximation, an analytical expression is found for the coefficient of transmission of photons through an array of QDs. It is shown that increasing the sensitivity of the SPT by increasing the number of QDs is possible only if the resonance condition for the transition frequencies is met for most of the QDs and the photon mode. This means that the choice of the initial parameters of the QD, which determine its individual frequency, must take into account and compensate the energy shift associated with other QDs. This shift depends on the array structure and the position of the given QD in it. An electron in the measured QD causes an additional shift, which violates the resonance of the frequencies of a certain number of QDs and the mode, thus changing the spectral response of the SPT. By analysing the frequency dependence of the response, it is possible to establish the presence or absence of an electron in the measured QD.

2. Model of an array of one-electron QDs interacting with the mode field of a photonic molecule in a steady-state pumping regime

The rapid development of solid-state nanophotonics, which emerged as an independent discipline in the first decade of the 21st century, made it possible to conduct systematic experimental studies of quantum optical nanostructures. As a result, measuring schemes were developed that allow the quantum state of a nanostructure (e.g., the electron population of a QD) to be determined by measuring the spectral dependence of the photon transmission coefficient through an MC that interacts with a QD [22]. One of the main parameters on which the accuracy of such a measurement depends is the interaction energy of the QD and the MC mode, which plays the role of the Rabi frequency of the energy quantum oscillations between them. The larger it is, the higher the measurement contrast and the signal-to-noise ratio. Its magnitude $\Omega_c = -\boldsymbol{E}_c \boldsymbol{d}/\hbar$ depends on the dipole moment $\boldsymbol{d}$ of the QD and the field strength $\boldsymbol{E}_c$ of the MC mode in the region where the QDs are located, as well as on their orientation. Both parameters have upper limitations related to fixed sizes of subsystems. The field amplitude (more precisely, its rms value $E_{rms} = \sqrt{\langle E_c^2 \rangle} = \sqrt{\hbar\omega_c/(2\varepsilon_0 \varepsilon V_c)}$, where ω_c is the MC frequency, ε_0 is the vacuum permittivity, and ε is the semiconductor permittivity) is estimated from the condition of normalising the electric field energy per photon:

$$\int \varepsilon_0 \varepsilon E_c^2 \mathrm{d}V = \hbar\omega_c/2$$

(below we put $\hbar \equiv 1$). The projection of the matrix element of the QD dipole moment operator on the direction of field polarisation can be estimated by the formula $d \approx -er$, where r is the mean QD radius, and e is the electron charge. Recall that the frequencies of the subsystems also depend on their size. Therefore, an increase in the QD radius in order to increase the dipole moment will be accompanied by a decrease in the transition frequency, and a decrease in the cavity volume V_c, which increases the field amplitude, will ultimately lead to 'pushing out' of all modes from the MC. It is interesting to note that for practically all known hybrid systems of the cavity + atom type, the Rabi frequency turns out to be of the order of the decay rate of a quantum state. As a rule, it is their ratio that indicates the possibility of implementing a particular regime and maintaining coherence.

Provided that for a given system the maximum possible value of Ω_c is reached, further optimisation will be associated with the suppression of dissipative effects by improving the quality of the material and manufacturing technology. However, there is also an alternative strategy that makes it possible to strengthen the coupling between the MC photon and matter. For this purpose, it is necessary to increase the number N of 'atoms' in the antinodes of the mode, which will lead to an increase in the effective Rabi frequency in proportion to $\sqrt{N}$. Obviously, such an enhancement will be noticeable only for a sufficiently large N: increasing the Rabi frequency by an order of magnitude requires putting 100 'atoms' inside the MR instead of one. If one of the 'atoms' is used as a quantum bit, then this approach may be unacceptable, since the addition of other 'atoms' will give rise to their unwanted interaction with the qubit. On the other hand, if the structure is used as a measuring system (quantum electrometer) that determines the presence or absence of an electron in a given region, then such optimisation looks very useful. Then the array of 'atoms' can be considered as an optically active sensory medium (antenna) when tracking the movement of an electron over short distances.

Let us consider the structure (Fig. 1) formed by two optical microcavities, MC1 and MC2, between which a coherent transfer of photons is possible. Such structures are sometimes referred to as photonic molecules (PMs) [23–25]. MC1 is used as an input port through which photons enter the structure. An array of one-electron QDs formed at the antinode of the mode field of MC2 (output port) is a quantum nonlinear medium that regulates photon transport through the structure. The detector picks up the emitted photons, which carry information about the state of the QD array. Therefore, by

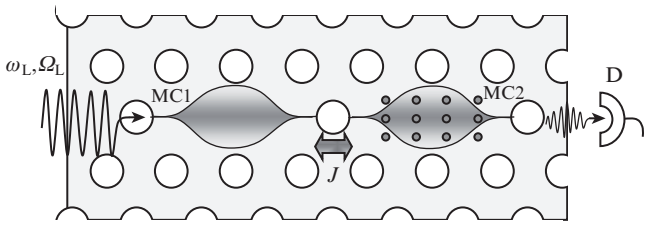

Figure 1. PM scheme with spatially separated input (MC1) and output (MC2) ports (defects in a lattice of holes in a two-dimensional photonic crystal). MC1 and MC2 are coupled due to photon tunnelling at a rate J. The QD array is located at the antinode of the MC2 mode. The system is pumped by a cw laser radiation with a frequency ω_L in a subphoton stationary regime at a rate Ω_L. The average number of transmitted photons is measured by a photodetector D located near MC2.

varying the frequency and amplitude of the external field, it is possible to study the spectral response of the electron–photon system. This design provides spatial separation of incident and transmitted photons, which increases measurement accuracy. Depending on the frequency detunings of the PM modes and the frequencies of electronic transitions in QDs, the process of photon transfer can be implemented in a resonant or dispersive regime.

In this paper, we study a one-dimensional array (chain) of QDs, formed inside an extended linear defect in the lattice of holes in a two-dimensional photonic crystal. The distance a_x between adjacent QDs is the same for the entire chain. We will assume that the centre of the first QD in the chain is aligned with the origin, and the centre of the tested QD has the coordinates L_x, L_y. Laser radiation with a frequency ω_L is focused on the MC1 surface. The rate Ω_L of the arrival of photons at the structure is determined by the degree of overlap of the fields of the MC1 mode and the laser radiation, as well as by its power. We will assume that the frequencies ω_{c1} and ω_{c2} of the MC1 and MC2 modes are close enough for the possibility of photon exchange between them. The rate J of photon exchange (tunnelling) is proportional to the overlap integral of the electromagnetic fields of their modes. Let MC2 contain N QDs, each having two electronic states (ground and excited). The ground state $|g_k\rangle$ of the QD with number k ($k = 1 - N$) has the energy ε_{gk}, and its excited state $|e_k\rangle$ has the energy ε_{ek}. The set of frequencies $\omega_k = \varepsilon_{ek} - \varepsilon_{gk}$ of electronic transitions characterises their spectral homogeneity. As a model, we choose a two-dimensional QD formed by an exponential-power potential [26],

$$U(x,y) = U_0 \exp[-(x/r_x)^{2p} - (y/r_y)^{2p}], \tag{1}$$

where U_0 is the QD depth; $2r_{x(y)}$ is the length of the QD along the direction of the $x(y)$ axis; and p is a parameter specifying the smoothness of the potential. Effective atomic units (e.a.u.) are used as units of measurement: 1 e.a.u. = $\mathrm{Ry}^* = m^*\mathrm{Ry}/(m_e\varepsilon^2)$ for energy and 1 e.a.u. = $a_B^* = a_B m_e \varepsilon/m^*$ for length, where Ry =13.6 eV is the Rydberg energy; $a_B = 0.52\times10^{-10}$ m is the Bohr radius; m_e is the mass of a free electron; and m^* is the effective mass of the electron. For gallium arsenide GaAs ($\varepsilon = 12$ and $m^* = 0.067m_e$), we have $\mathrm{Ry}^* = 6$ meV and $a_B^* = 10$ nm. Let us choose the parameters of the QD potential (1) as follows: $r_x = 0.7$, $r_y = 0.8$, $U_0 = -22$, and $p = 5$. Then the frequency of the transition between the ground and excited states of the QD is 9.92 e.a.u.

The energy of the Coulomb interaction of two electrons localised in the ground states of QDs with numbers k and m,

$$V(g_k,g_m) = 2\iint \mathrm{d}\boldsymbol{r}_k \mathrm{d}\boldsymbol{r}_m \left|\Psi_g(\boldsymbol{r}_k)\right|^2 \left|\Psi_g(\boldsymbol{r}_m)\right|^2 / \left|\boldsymbol{r}_k - \boldsymbol{r}_m\right|, \tag{2}$$

where $\boldsymbol{r}_{k(m)}$ is the radius vector of the electron in the QD number k (m). The energy of the Coulomb interaction of two electrons, one of which is in the ground state of the QD number k and the other in the excited state of the QD number m, is expressed as

$$V(g_k,e_m) = 2\iint \mathrm{d}\boldsymbol{r}_k \mathrm{d}\boldsymbol{r}_m \left|\Psi_g(\boldsymbol{r}_k)\right|^2 \left|\Psi_e(\boldsymbol{r}_m)\right|^2 / \left|\boldsymbol{r}_k - \boldsymbol{r}_m\right|. \tag{3}$$

The matrix elements (2) and (3) are diagonal components of the Coulomb interaction Hamiltonian and are included in the energy levels of the two-electron system. We do not consider configurations with double population of one QD, assuming that the corresponding addition to the energy of the excited level will lead to its pushing out into the continuous spectrum of the conduction band (ionisation). Let us calculate the energies of three possible two-electron configurations: $V(g_k,g_k) = 4.22$, $V(g_k,e_k) = 3.22$, $V(e_k,e_k) = 2.99$. Each of them is higher than the ionisation energy (~2.61). We also neglect the tunnel coupling between neighbouring QDs, choosing the thickness and height of the barrier separating them sufficiently large. Electrons can make independent resonant transitions between the states $|g_k\rangle$ and $|e_k\rangle$ of the kth QD, exchanging an energy quantum with the PM mode with the Rabi frequency Ω_k ($k = 1 - N$). In the absence of interaction (for example, if the distance between QDs is large compared to their size), the spectrum of the electron-photon system is represented by a set of Tavis–Cummings polariton modes [27]. Its difference from the better-known Jaynes–Cummings spectrum, which describes a particular case with one QD, is that the states of the electronic subsystem are now represented by superpositions of all singly excited states of the QD array. When the frequencies of all QDs are equal, only two extreme (upper and lower) modes are optically active (the so-called 'light' modes), and the remaining $N-2$ modes turn out to be 'dark', not revealing themselves during spectroscopic measurements.

We will assume that no more than one excitation quantum is present in the structure. Then the Hamiltonian of the system has the form:

$$\begin{aligned} H = {} & \omega_{c1} a_1^\dagger a_1 + \omega_{c2} a_2^\dagger a_2 + J(a_1^\dagger a_2 + a_2^\dagger a_1) \\ & + \sum_{k=1}^{N} \varepsilon_{gk} |g_k\rangle\langle g_k| + \sum_{k=1}^{N} \varepsilon_{ek} |e_k\rangle\langle e_k| \\ & + \sum_{k>m} V(g_k,g_m) |g_k g_m\rangle\langle g_k g_m| \\ & + \sum_{k>m} V(g_k,e_m) |g_k e_m\rangle\langle g_k e_m| \\ & - \sum_{k=1}^{N} \Omega_k (|e_k\rangle\langle g_k| a_2 + |g_k\rangle\langle e_k| a_2^\dagger) \\ & + 2\Omega_L \cos(\omega_L t)(a_1^\dagger + a_1). \end{aligned} \tag{4}$$

Here a_1 and a_2 are the operators of annihilation of a photon in the MC1 and MC2 modes, respectively, and for describing the energy exchange between QD and MC2, the rotating wave approximation is used, which assumes the fulfilment of the conditions $\omega_k \gg \Omega_k$. The dimension of the space of basis vectors is equal to N+3. The vectors

$$|1\rangle = |g_1,\ldots,g_N\rangle|00\rangle, \quad |2\rangle = |g_1,\ldots,g_N\rangle|10\rangle,$$

$$|3\rangle = |g_1,\ldots,g_N\rangle|01\rangle$$

describe the vacuum state of the electron–photon system and the states corresponding to the presence of one photon in the modes of MC1 and MC2, respectively. The remaining vectors $|k+3\rangle = |g_1,\ldots,e_k,\ldots,g_N\rangle|00\rangle$ ($k = 1 - N$) describe the excitation of an electron in the kth QD. The state vector

$$|\Psi\rangle = \sum_{k=1}^{N+3} c_k |k\rangle$$

of the system is represented as an expansion in basis vectors with time-dependent coefficients c_k. The evolution of the state vector obeys the Schrödinger equation $i\partial_t|\Psi\rangle = H|\Psi\rangle$ with the initial condition $|\Psi(0)\rangle = |1\rangle$.

If the laser operates in a cw regime, then by applying the transformation

$$T = \exp\left[-i\omega_L t\left(a_1^\dagger a_1 + a_2^\dagger a_2 + \sum_{k=1}^{N}|e_k\rangle\langle e_k|\right)\right]$$

to the Hamiltonian H, we can eliminate its time dependence. In this case, the frequencies of the MC and QD modes are shifted by the laser radiation frequency ω_L. In addition, it is necessary to take into account the incoherent processes of photon dissipation associated with the uncontrolled energy transfer from MC1 and MC2 into the continuum with the rates κ_1 and κ_2, and the electronic relaxation with the rate γ_k due to the interaction of the kth QD with the phonon environment. A rigorous consideration of these phenomena is possible only within the framework of the density matrix formalism and the Lindblad equation (see below); however, an approximate solution, valid for a small probability of the system excitation from a vacuum state, can be found using a simpler formalism of the Schrödinger equation. To do this, in Eqn (4), one should replace $\omega_{c1(2)} \to \omega_{c1(2)} - i\kappa_{1(2)}$ and $\omega_k \to \omega_k - i\gamma_k$.

Let us choose the value

$$\varepsilon^{(0)} = \sum_{k=1}^{N}\varepsilon_{gk} + \sum_{m>k}V(g_k,g_m)$$

as zero for the energy and introduce the frequency shift

$$G_k = \sum_{m\neq k}[V(e_k,g_m) - V(g_k,g_m)]$$

of the kth QD. This parameter characterises the non-equivalence of the Coulomb interaction of an electron in the ground and in excited states of the kth QD with the electrons of the remaining QDs in the ground state. Then the Schrödinger equation, with the above transformations taken into account, turns out to be identical to the system of differential equations for the probability amplitudes of the basis vectors in the expansion of the state vector:

$$i\partial_t\begin{pmatrix} c_1\\ c_2\\ c_3\\ c_4\\ \dots\\ c_{N+3}\end{pmatrix} =$$

$$\begin{pmatrix} 0 & \Omega_L & 0 & 0 & \dots & 0\\ \Omega_L & \delta_{c1}-i\kappa_1 & J & 0 & \dots & 0\\ 0 & J & \delta_{c2}-i\kappa_2 & -\Omega_1 & \dots & -\Omega_N\\ 0 & 0 & -\Omega_1 & \delta_1+G_1-i\gamma_1 & \dots & 0\\ \dots & \dots & \dots & \dots & \dots & \dots\\ 0 & 0 & -\Omega_N & 0 & \dots & \delta_N+G_N-i\gamma_N\end{pmatrix}$$

$$\times\begin{pmatrix} c_1\\ c_2\\ c_3\\ c_4\\ \dots\\ c_{N+3}\end{pmatrix}, \qquad (5)$$

where $\delta_{c1(2)} = \omega_{c1(2)} - \omega_L$ is the detuning of the frequency of MC1(2) and $\delta_k = \omega_k - \omega_L$ is the detuning of transitions in a QD from the frequency of laser radiation. To calculate G_k ($k = 1 - N$) for a linear array consisting of identical QDs, it is sufficient to plot the difference $\Delta V = V(e_k,g_m) - V(g_k,g_m)$, versus the distance between the centres of two QDs. Then, knowing the configuration of the array (i.e., the coordinates of the centres of all QDs), it is easy to find all quantities entering Eqn (5).

Let us obtain an approximate solution of system (5) in the steady-state regime of subphoton pumping, when $c_1 \approx 1$ and $\partial_t c_k = 0$. This regime is achieved in a time $t_{ss} \gg 1/\kappa_2$, which exceeds the characteristic time of photon dissipation. We will be interested in the average population $\langle n_2\rangle = |c_3(t_{ss})|^2$ of the MC2 mode, which determines the transmission coefficient, i.e., the number of photons passing through the SPT from the source to the detector. A system of N+3 homogeneous differential equations is reduced to an inhomogeneous algebraic system of N+2 equations, solving which, we find an expression for the population of the MC2 mode:

$$\langle n_2\rangle \approx \frac{\Omega_L^2 J^2|F|^2}{\left|[(\delta_{c1}-i\kappa_1)(\delta_{c2}-i\kappa_2)-J^2]F-(\delta_{c1}-i\kappa_1)\sum_{m=1}^{N}\Omega_m^2 F_m\right|^2}, \qquad (6)$$

where

$$F_m = \prod_{k\neq m}^{N}(\delta_k + G_k - i\gamma_k), \quad F = \prod_{k=1}^{N}(\delta_k + G_k - i\gamma_k)$$

are products of the QD array resonant denominators. In the absence of interaction between the QD and the MC2 mode ($\Omega_m = 0$), the denominator of Eqn (6) has two minima corresponding to the frequencies of the PM modes, which are formed due to the tunnelling of photons between MC1 and MC2 at non-zero J. To achieve the maximum value of the collective Rabi frequency, it is necessary to adjust the frequencies of transitions of all QDs of the array to resonance with the frequency of one of the PM modes. Let us choose as such a mode a symmetric PM mode (provided that $\delta_{c1} \approx \delta_{c2}$) having a frequency $\omega_{PM-} = \omega_{c2} - J$. The amplitudes of both PM modes in MC2 turn out to be $\sqrt{2}$ times less than the amplitude of the isolated MC2 mode due to renormalisation associated with an increase of the system optical volume by two times. Therefore, all Rabi frequencies will also be $\sqrt{2}$ times less than the Ω_k values. If the detuning of the transition frequency in the kth QD, caused by the Coulomb interaction with other QDs, turns out to be equal to or greater than the coupling energy of the QD and the mode, $|G_k| \geqslant \Omega_k$, then the energy exchange between the QD and the mode becomes ineffective. Nevertheless, even in this case, the QD affects the transport properties of the PM, generating a dispersion shift of mode frequency. By setting the parameters of the QD potential in such a way that the condition $\omega_k = \omega_{PM-}$

– G_k is satisfied, we compensate for the Coulomb detuning, restoring the resonance nature of the interaction.

How should the density of a QD array be chosen? To achieve a noticeable increase in its effect on the transmission of photons in comparison with a single QD, the number N of QDs must satisfy the condition $\Omega_c\sqrt{N} \geqslant \kappa_{1,2}$. This will allow high resolution of peaks even at moderate Q-factor of the MC. In this case, it is necessary to take into account the finiteness of the mode volume, as a result of which an increase in N will inevitably be associated with a decrease in the distance between neighbouring QDs and an increase in the role of Coulomb effects. In addition, the dimensions of the MC itself determine its spectrum, the increase in volume is accompanied by a decrease in the frequencies and amplitudes of the MC mode fields, and in this sense it is undesirable. Finally, since QDs are host implantation defects with respect to the MC material [28], they will negatively affect its optical properties, deteriorating the mode Q-factor. Therefore, the total volume of all QDs in the array should be significantly less than the mode volume: $N\langle V_a\rangle \ll V_c$, where $\langle V_a\rangle$ is the average volume of the QD.

3. The role of Coulomb effects in the steady-state dynamics of a QD array

As we have already mentioned, in compact many-electron systems, the influence of Coulomb effects on the spectrum and on the dynamics of an ensemble of electrons noticeably increases with decreasing distance between QDs. In addition to the energy level shifts, described by the diagonal components of Hamiltonian (4) and caused by the difference in the distributions of the electron density of the QD in its ground and excited states, when the QDs approach to a distance of the order of their radius, off-diagonal Coulomb matrix elements begin to play a significant role. They determine the rates of dynamic processes that cause transitions between stationary states of the system. Coherent resonant transfer of excitation between QDs without moving an electron (exciton) is considered the most important of them. This phenomenon is known as the Förster effect [29–31]. The rate of this process is determined by the matrix element

$$V_{km}^{F} = 2\iint \mathrm{d}\boldsymbol{r}_k \mathrm{d}\boldsymbol{r}_m \Psi_g^*(\boldsymbol{r}_k)\Psi_e^*(\boldsymbol{r}_m)\Psi_g(\boldsymbol{r}_m) \times \Psi_e(\boldsymbol{r}_k)/|\boldsymbol{r}_k - \boldsymbol{r}_m|, \quad (7)$$

and the corresponding Hamiltonian has the form

$$H_F = \sum_{k\neq m} V_{km}^{F} |g_k e_m\rangle\langle e_k g_m| + \text{h.c.} \quad (8)$$

Thus, the Förster dynamics is represented by two synchronous optical transitions $|e_k\rangle \rightleftarrows |g_k\rangle$ in the kth QD and $|g_m\rangle \rightleftarrows |e_m\rangle$ in the mth QD, occurring in opposite directions. This process will be effective only if the transition frequencies in both QDs are close, i.e., when the condition of their resonance is satisfied, $|\omega_k - \omega_m| \ll |V_{km}^{F}|$. Another Coulomb process, the energy of which is expressed by matrix elements of the form

$$V_{km}^{(ge,g)} = 2\iint \mathrm{d}\boldsymbol{r}_k \mathrm{d}\boldsymbol{r}_m \Psi_g^*(\boldsymbol{r}_k)\Psi_g^*(\boldsymbol{r}_m)\Psi_e(\boldsymbol{r}_k) \times \Psi_g(\boldsymbol{r}_m)/|\boldsymbol{r}_k - \boldsymbol{r}_m|, \quad (9)$$

is the transition from the excited state to the ground state of one QD, induced by the field of an electron in another QD. The corresponding Hamiltonian should be supplemented with a Hermitian-conjugate expression describing the inverse process:

$$H_{\text{nondiag}}^{(ge,g)} = \sum_{k\neq m} V_{km}^{(ge,g)} |g_k g_m\rangle\langle e_k g_m| + \text{h.c.} \quad (10)$$

In contrast to the Förster resonant energy exchange, in this process the energy is not conserved, and, therefore, it is virtual, leading only to a small shift of the QD frequencies, $|V_{km}^{(ge,g)}/\omega_{k(m)}| \ll 1$. Dependences of the Stark frequency shift ΔV and the Förster energy V_F on the distance between QDs with the parameters indicated above are shown in Fig. 2. It is seen that the moduli of these energies rapidly increase with decreasing distance L between QDs.

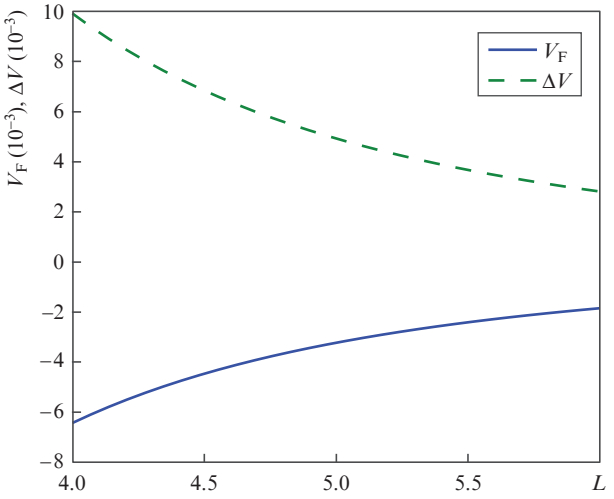

Figure 2. Dependences of the Stark ΔV and Förster V_F energies for two identical one-electron QDs with the parameters of the potential $r_x = 0.7$, $r_y = 0.8$, $U_0 = -22$, $p = 5$ on the distance L between the QD centres. The centres of the QDs lie on the x axis in the xy plane, and the angles of rotation of the QDs around their axial axes are equal to zero. Configuration of excited orbitals p_x–p_x. All values are given in e.a.u. for gallium arsenide.

Another feature of the matrix elements is associated with their angular dependences. If the distance between the QDs is fixed and the angles φ_1 and φ_2 of the QD rotations around the axes passing through their centres vary, then the Coulomb energies will also change. It is easy to see (Fig. 3) that upon rotation through the angle $\varphi_2 = \pi/2$ (i.e., upon transformation of the wave function of the excited state p_x of QD 2 into p_y), the G_2 shift becomes negative, and the Förster energy becomes zero. Therefore, in this way it is possible to regulate their influence on the dynamics of the system at a fixed number of QDs and the distance between their centres. In particular, alternating the excited p_x and p_y orbitals of neighbouring QDs in a one-dimensional chain, one can largely suppress the Förster effect.

What is the role of Coulomb effects in the steady-state dynamics of PM and QD array? To answer this question, a deeper study is needed, which requires the use of the density matrix formalism. The dynamics of an electron–photon system is described by the Lindblad equation, the solution of

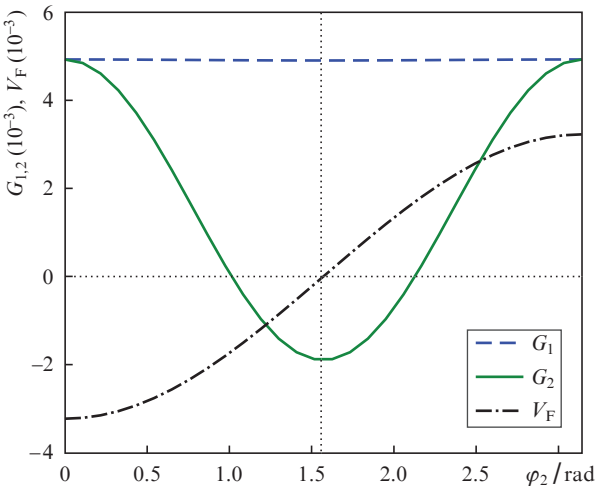

Figure 3. Dependences of the Stark shifts of QD 1 (G_1) and QD 2 (G_2) and the Förster energy V_F on the angle φ_2 of rotation of QD 2 around the z axis passing through its centre for a distance $L = 5$ between the centres of the QDs. All energy quantities are given in e.a.u. for gallium arsenide.

which gives the time dependence of its density matrix ρ for a given initial state $\rho(0)$:

$$\frac{d\rho}{dt} = -i[H + H_F,\rho] + \sum_{k=1}^{2}\kappa_k D(a_k) + \sum_{k=1}^{N}\gamma_k D(|g_k\rangle\langle e_k|) + \sum_{k=1}^{N}\gamma_{dk} D(|e_k\rangle\langle e_k| - |g_k\rangle\langle g_k|), \quad (11)$$

where γ_{dk} is the rate of electron dephasing in the kth QD. Dissipative photonic and electronic processes are modelled by the Lindblad operators $D(O) = O\rho O^{\dagger} - [O^{\dagger}O,\rho]/2$. Let us find a steady-state solution of Eqn (11) for a linear structure of four one-electron QDs in a vacuum state, assuming that the laser exposure time exceeds the relaxation time of the system.

We start with the case when the excited orbitals of all QDs are oriented along the structure axis (configuration p_x–p_x–p_x–p_x). For the convenience of comparing the exact solution with the analytical approximation (6), both solutions are presented in Fig. 4. As we have already found out, the Coulomb interaction causes shifts of the transition frequencies in the QD, depending on its position in the structure. If the distance between neighbouring QDs is comparable to their size, then the shifts bring the QD out of resonance with the PM mode, shifting the frequency of the peak. It is logical to assume that an increase in the distance will lead to a weakening of the Coulomb interaction and a gradual restoration of the resonance (doublet) shape of the spectral curve. The results of calculations shown in Fig. 4a fully confirm this assumption: with increasing distance a_x, the doublet structure of the response is restored, and with a significant distance between QDs ($a_x > 80$ nm), it tends to the dependence for a PM with noninteracting QDs. Comparison of the exact numerical solution found with allowance for off-diagonal Coulomb effects and QD dephasing with the approximate solution (6) indicates some difference in the frequencies and widths of the resonance peaks. To understand which of the effects not taken into account in equation (6) has the greatest

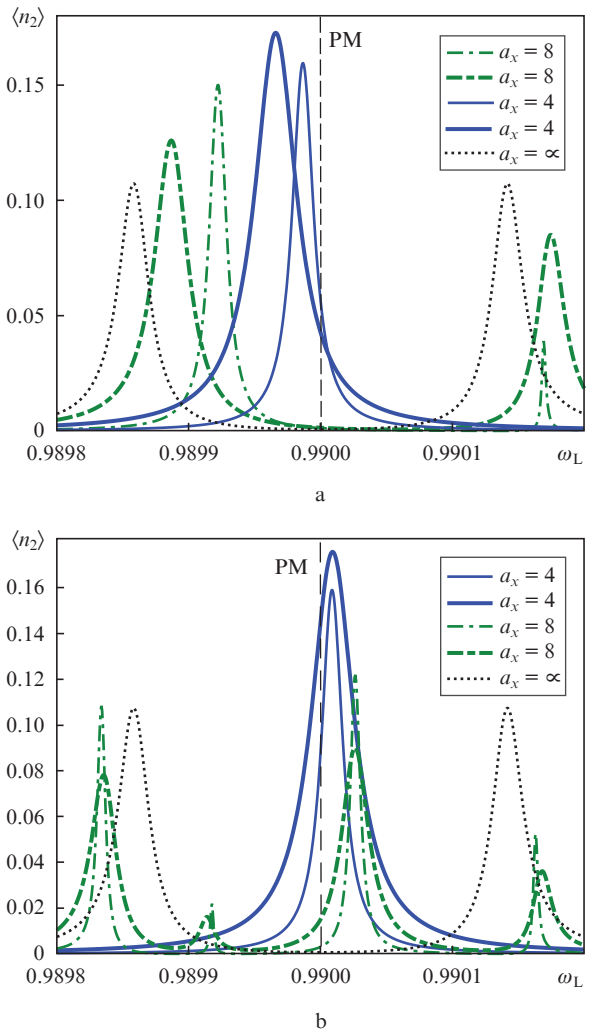

Figure 4. Spectral responses of PM with a linear chain of four QDs without Coulomb shifts compensation for two values of the chain period a_x, obtained by solving the Lindblad equation (thick curves) and using an approximate formula (thin curves). Chains with homogeneous (a) and optimised (b) sequences of excited orbitals are considered. The position of an even PM mode without QDs is indicated by a vertical dashed line. For comparison, the dependence of the PM response with noninteracting (infinitely distant) QDs is shown. The system parameters are $J = 0.01$, $\Omega_L = 8 \times 10^{-6}$, $\Omega_c = 10^{-3}$, $\delta_{c1(2)} = \delta_k = 0$, $\gamma_k = \gamma = 10^{-6}$, $\gamma_{dk} = \gamma_d = 0.5\gamma$, $\kappa_{1,2} = 10^{-5}$. All energy quantities are given in units of MC1 frequency, distances are given in e.a.u.

influence on the spectral curve, we use the result shown in Fig. 3. When one of the QDs is rotated by an angle $\pi/2$ around its axis, the Förster energy becomes zero. If the chain is formed by alternating QDs with excited p_x and p_y orbitals (configuration p_x–p_y–p_x–p_y), then the Förster energy exchange between neighbouring QDs will be suppressed. In this case, the calculation results demonstrate a good agreement between the resonance frequencies for the exact and approximate solutions, indicating that the Förster interaction is the main source of frequency shifts in the homogeneous chain. Dephasing caused by stochastic fluctuations of the transition frequencies in QDs and not taken into account in the approximate approach of the Schrödinger equation leads to additional broadening of the peaks. At the same time, for an inhomogeneous QD chain, with an increase in the distance a_x, two

more resonance peaks appear, which are not present in the dependences for a homogeneous QD chain (Fig. 4b). Since they are present both on the analytical and on the numerically calculated curve, their origin is unambiguously associated with the diagonal matrix elements of the Coulomb interaction.

Using the point charge approximation, we calculate the values of G_k at each QD. For a homogeneous chain, we obtain the set $G_1 = G_4 \approx r_p^2/(2a_x^3)$, $G_2 = G_3 \approx r_p^2/a_x^3$ (in e.a.u., taking into account the interaction of only neighbouring QDs). The set for a nonuniform chain looks like this: $G_1 \approx r_p^2/(2a_x^3)$, $G_2 \approx -r_p^2/(2a_x^3)$, $G_3 \approx r_p^2/a_x^3$, and $G_4 \approx -r_p^2/(4a_x^3)$, indicating lower shear symmetry compared to a homogeneous chain. The analytical values are in good agreement with those found numerically (compare with Fig. 2) if we put $r_p \approx r_x/2 = 0.35$ (the coordinate of the maximum of the function $|\Psi_e(x,y)|^2$ on the x axis). In the case $a_x = 8$, we obtain $G_{1(4)} = 0.0012$, $G_{2(3)} = 0.0025$ for a homogeneous chain and $G_1 = 0.0012$, $G_2 = -0.0011$, $G_3 = 0.0025$, $G_4 = -0.0006$ for an inhomogeneous one. Since the energy parameters in Fig. 4 are taken in units of frequency ω_{c1} of MC1, the values of G_k must be converted from effective atomic units to the indicated units by multiplying by the ratio $\omega_{c1}/1$ e.a.u. ≈ 10. It is seen that these values satisfy the conditions $|G_k| \geqslant \Omega_k$, and this indicates that the system is in the resonant-dispersive regime, in which the electron–photon spectrum differs significantly from the resonance spectrum of the Tavis–Cummings model with two 'bright' states. However, only for an inhomogeneous chain, all four polariton modes have an optically active component due to the asymmetry of the shifts. In the next section, we will define the contrast of the PM measurement and study how the response and contrast depend on the distance to the QD under test.

4. Spectral response of a PM with a one-dimensional array of QDs

The above calculations indicate a significant influence of Coulomb effects inside the QD chain on the population of the PM transport mode, which is proportional to the average number of photons at the exit from the structure. The same feature makes it possible to determine the amount of charge in a QD located outside the MC and, therefore, optically inactive. The influence of the measured QD with number s on the kth QD of the array is expressed in an additional shift of its frequency by δV_{ks}, where $\delta V_{ks} = V(e_k, g_s) - V(g_k, g_s)$. In turn, these shifts in the QD frequencies cause a shift in the photon population peak, which can be easily found by comparing with the response of the structure in the absence of the measured QD (thick curve in Fig. 5). We define the measurement contrast as follows:

$$S = \max(|\langle n_2^{(0)}\rangle - \langle n_2^{(1)}\rangle|), \qquad (12)$$

where $\langle n_2^{(0)}\rangle$ is the average number of photons if there are no electrons in the measured QD, and $\langle n_2^{(1)}\rangle$ is the average number of photons if there is one electron in the QD. The maximum value of the mode population difference (12) is attained at the frequency of the spectral peak of the PM, which does not interact with the measured QD. After multiplying by the mode frequency, the quantity S will have the dimension of energy, which is convenient for estimating the power of the flux of transmitted photons, which is important for choosing the distance from the PM to the detector. The answer to the

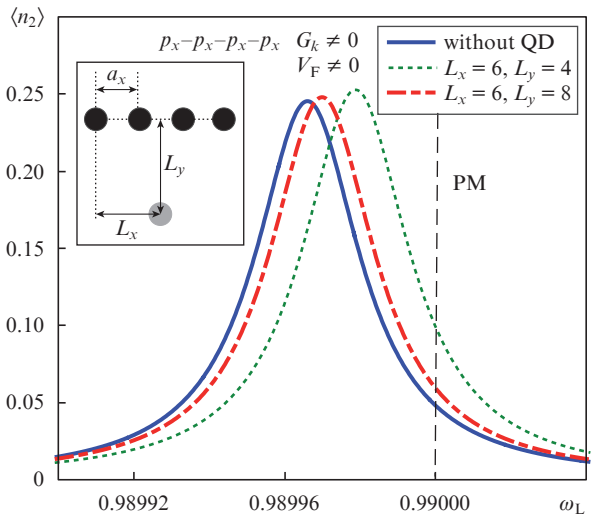

Figure 5. Spectral responses of a PM containing a chain of four QDs with a period of $a_x = 4$ for two positions of the measured QD centre (dispersion regime). The inset shows the geometry of the measuring circuit. The vertical dashed line marks the position of an even PM mode without a QD chain. The structure parameters are the same as for Fig. 4.

question of what position of the measured QD relative to the structure will be optimal is far from obvious. On the one hand, the closer the QD to a certain part of the chain, the more active its interaction with the electrons of several nearby QDs in comparison with other (more distant) QDs. This makes it possible to further suppress the electron–photon interaction between the mode and such QDs and thereby change the PM response. On the other hand, a QD located at a distance exceeding the characteristic size of the structure equally (but with much lower energy) interacts with all QDs of the array. Thus, the first configuration leads to almost complete optical blockade of the group of QDs, slightly affecting the rest of the array. For the second configuration, the frequency shifts in all QDs are approximately the same, but small. Which of the options turns out to be more effective will depend on the rest of the system parameters. The enhancement of the Coulomb interaction between the structure and the outer QD, as well as the suppression of electron–electron correlations in the structure, should be considered as natural steps towards optimising the response. This is achieved by external electrostatic control of the QD potential or by engineering the growth process of QD crystallites in order to select such chain parameters, at which all structural shifts of QD frequencies are exactly compensated by internal Coulomb shifts. In this case, the resonant character of the interaction with the PM mode is restored. Another important optimisation step is the suppression of the Förster exchange, which destroys the doublet structure of the response, by alternating the excited states of QDs with different symmetry (Fig. 6).

Figure 7 shows the dependences of the contrast S on the position L_x of the measured QD along the chain for two values of L_y at different degrees of compensation for Coulomb effects. For a structure without compensation, the contrast decreases rather rapidly with increasing distance L_y, in accordance with the dependences of the spectral response shown in Fig. 5. Whereas at $L_y = 4$ the contrast level is comparable to the level of the signal itself, at $L_y = 8$ it sharply decreases, making the described method of indirect measurement ineffective. Compensation of frequency shifts while maintaining

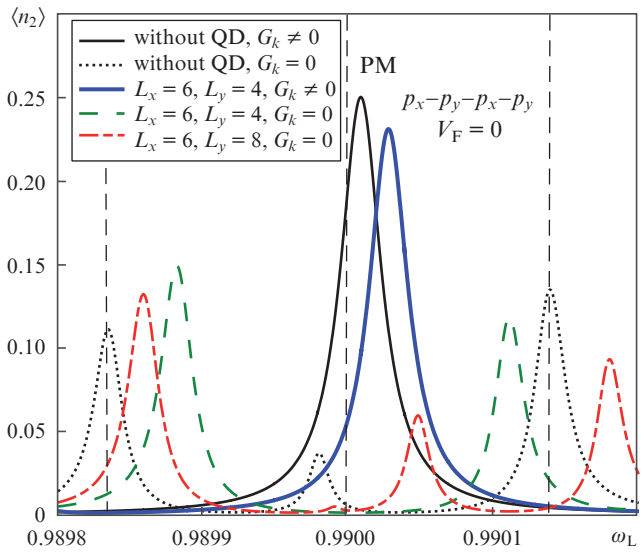

Figure 6. Spectral responses of a PM containing a chain of four QDs with a period of $a_x = 4$ for two positions of the centre of the measured QD (resonance regime). Vertical dashed lines mark the position of an even PM mode without QDs. The structure parameters are the same as for Fig. 4.

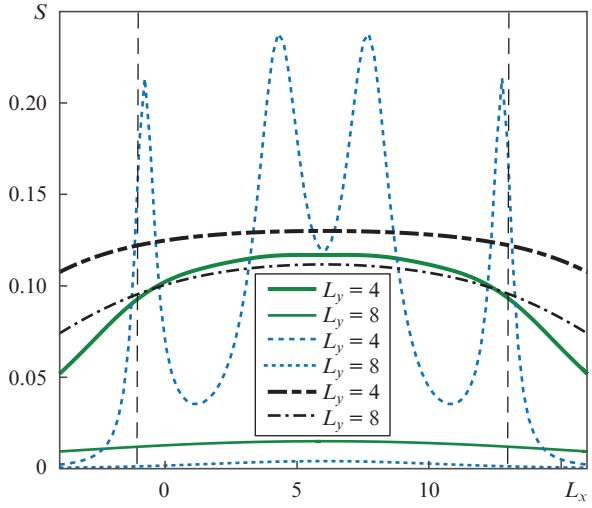

Figure 7. Dependences of the measurement contrast S of the structure on the horizontal position L_x of the external QD for two values of its vertical coordinate $L_y = 4$ and 8. Data are presented for structures without compensation for internal Coulomb effects (solid curves), as well as with partial (dashed curves) and complete (dash-dotted curves) compensation. Vertical dashed lines mark the effective boundaries of the structure. All values are given in e.a.u.

the Förster interaction significantly improves the efficiency of the procedure for the region near the chain ($1 < L_y < 6$); however, when the QD is vertically removed by a distance of $L_y > 8$, the contrast again decreases to zero. Note the presence of four local maxima for the curve with $L_y = 4$, which are absent in analogous curves with uncompensated and fully compensated electron interaction within the structure. Therefore, they are associated with the Förster effect. As we already know, the compensation of the latter requires splitting the QD chain into two sublattices differing in the orientation of the excited state orbitals (for example, p_x for odd QDs and p_y for even QD numbers). Full compensation of the Coulomb interaction makes it possible to slow down the decrease in contrast with an increase in the vertical displacement of the QD and to increase the resolution. This makes it possible to place a qubit at a greater distance than for a structure without compensation.

To construct the coordinate dependence of the contrast $S(L_x, L_y)$ in the half-plane, we use Eqn (6), the application of which yields the correct result for QD chains with suppressed Förster interaction and with low rates of QD dephasing, which is mainly associated with acoustic phonons. The obtained two-dimensional picture (Fig. 8) reflects the general trend of a smooth decrease in contrast with the distance of the measured QD from the chain. Its location in the region $0 < L_x < 4a_x$ guarantees reliable measurement at significant vertical distances. On the contrary, placing the measured QD on the x axis leads to a rapid decrease in contrast already at a small distance from the boundaries of the chain.

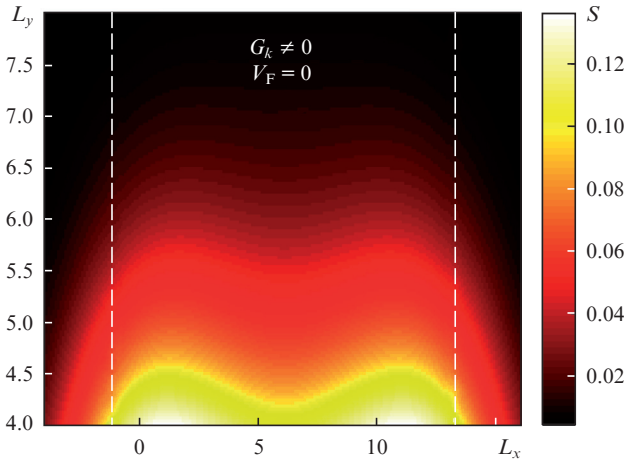

Figure 8. Spatial dependence of the contrast $S(L_x, L_y)$ on the coordinates of the centre of the measured QD without compensation for the Coulomb frequency shifts of the QD chain. Vertical dashed lines indicate the effective chain boundaries. All values are given in e.a.u.

The results presented in Figs 7 and 8 allow formulating general recommendations for optimising the measurement. It is desirable to position the tested object so that the distance to all QDs of the chain is approximately the same (the area in Fig. 8, bounded by vertical dashed lines). To maintain high contrast values upon moving QDs at a large distance ($L_y > 10$), it is necessary to compensate the Coulomb frequency shifts of optical transitions in the QD chain and to minimise the Förster interaction between them. Compensation can be implemented by properly choosing the shape of the QD potential and the distance between adjacent QDs, depending on their position in the array. It does not require additional infrastructure (a set of gate electrodes). In other words, filling all the QDs of the array with electrons should restore the resonance of the QD and mode frequencies due to mutual compensation of structural and Coulomb shifts equal in magnitude but opposite in sign. As you might guess, the values of the Coulomb shifts will be larger for QDs located in the central region of the array; therefore, both the distance to neighbouring QDs and the depths of their potentials should be greater. However, a structure exists that does not require additional engineering of QD potentials to implement this approach. These are QDs evenly spaced on a circle. In this

case, due to the equivalence of the Hamiltonians for each QD, their frequency shifts due to the electron-electron interaction will be similar. The electron in the measured QD on the axial axis passing through the centre of the circle also equally affects each of the QDs of the annular array. This should facilitate a synchronous exit from resonance with the mode of all QDs in the array when this QD is populated, which will be accompanied by a sharp change in the spectral response (restoration of the 'empty' PM spectrum). As a final remark, let us point out the need to maintain the subphoton regime conditions, in which the average number of photons of the mode does not exceed unity [32].

5. Conclusions

In this paper, we analyse the possibility of using a one-photon scheme for spectroscopic monitoring of the state of charged nano-objects. A method is proposed for optical measurement of the population of QDs located at a considerable distance from the device. Our method is consistent with the quantum measurement scheme using the Jaynes–Cummings effect, supplementing it with some new details. In particular, we prove that it is necessary to correctly take into account the Coulomb interaction, when, in addition to the Stark (diagonal) shifts of the QD frequencies, the Hamiltonian also contains off-diagonal components describing the Förster effect. The PM response (the average number of photons at the exit from the structure) depends on the observance of the conditions for the resonance of the QD array and the PM transport mode. An increase in the number of QDs leads to an increase in the energy of collective electron-photon interaction, restoring the resolution of spectral lines for PM with a low Q-factor. However, if the density of QDs in the array is high, then the Stark shifts and the Förster effect suppress the resonant exchange of a quantum between the QD and the mode, transferring the OPT to the dispersive regime, which is characterised by low sensitivity. Thus, there are ways to optimise the measurement process associated with structural engineering. In particular, the individual choice of the QD potentials and the array geometry, at which the resonance of the frequencies of all QDs and the PM mode is restored, provides the maximum measurement contrast.

Acknowledgements. The investigation was supported by Program No. 0066-2019-0005 of the Ministry of Science and Higher Education of Russia for the Valiev Institute of Physics and Technology of RAS.

References

1. Joyce B.A., Kelires P.C., Naumovets A.G., Vvedensky D.D. *Quantum Dots: Fundamentals, Applications, and Frontiers* (Dordrecht: NATO Science Series, 2003).
2. Michler P. *Single Semiconductor Quantum Dots* (Springer, 2009).
3. Coe-Sullivan S. *Nat. Photonics*, **3**, 315 (2009).
4. Ono Y., Fujiwara A., Nishiguchi K., Inokawa H., Takahashi Y. *J. Appl. Phys.*, **97**, 031101 (2005).
5. Gustavsson S., Leturcq R., Ihn T., Ensslin K., Gossard A.C. *J. Appl. Phys.*, **105**, 122401 (2009).
6. Fedichkin L., Yanchenko M., Valiev K.A. *Nanotechnology*, **11**, 387 (2000).
7. Hayashi T., Fujisawa T., Cheong H.D., Jeong Y.H., Hirayama Y. *Phys. Rev. Lett.*, **91**, 226804 (2003).
8. Gorman J., Hasko D.G., Williams D.A. *Phys. Rev. Lett.*, **95**, 090502 (2005).
9. Sherwin M.S., Imamoglu A., Montroy T. *Phys. Rev. A*, **60**, 3508 (1999).
10. Tsukanov A.V. *Phys. Rev. A*, **85**, 012331 (2012).
11. Barthel C., Kjærgaard M., Medford J., Stopa M., Marcus C.M., Hanson M.P., Gossard A.C. *Phys. Rev. B*, **81**, 161308(R) (2010).
12. Simmons C.B., Thalakulam M., Shaji N., Klein L.J., Qin H., Blick R.H., Savage D.E., Lagally M.G., Coppersmith S.N., Eriksson M.A. *Appl. Phys. Lett.*, **91**, 213103 (2007).
13. Kimble H. *Nature*, **453**, 1023 (2008).
14. Nielsen M.A., Chuang I.L. *Quantum Computation and Quantum Information* (Cambrige: Cambrige University Press, 2000).
15. Tsukanov A.V. *Quantum Electron.*, **51**, 84 (2021) [*Kvantovaya elektronika*, **51**, 84 (2021)].
16. Walmsley A. *Science*, **348**, 525 (2015).
17. Schneider C., Huggenberger A., Sünner T., Heindel T., Strauss M., Göpfert S., Weinmann P., Reitzenstein S., Worschech L., Kamp M., Höfling S., Forchel A. *Nanotechnology*, **20**, 434012 (2009).
18. Kiravittaya S., Benyoucef M., Zapf-Gottwick R., Rastelli A., Schmidt O.G. *Appl. Phys. Lett.*, **89**, 233102 (2006).
19. Mano T., Nötzel R., Zhou D., Hamhuis G.J., Eijkemans T.J., Wolter J.H. *J. Appl. Phys.*, **97**, 014304 (2005).
20. Van Lippen T., Nötzel R., Hamhuis G.J., Wolter J.H. *J. Appl. Phys.*, **97**, 044301 (2005).
21. Zhang L., Teng C.-H., Hill T.A., Lee L.-K., Ku P.-C., Deng H. *Appl. Phys. Lett.*, **103**, 192114 (2013).
22. Stumpf W.C., Asano T., Kojima T., Fujita M., Tanaka Y., Noda S. *Phys. Rev. B*, **82**, 075119 (2010).
23. Morichetti F., Ferrari C., Canciamilla A., Melloni A. *Laser Photonics Rev.*, **6**, 74 (2012).
24. Ohta R., Ota Y., Nomura M., Kumagai N., Ishida S., Iwamoto S., Arakawa Y. *Appl. Phys. Lett.*, **98**, 173104 (2011).
25. Zhu W., Wang Z.H., Zhou D.L. *Phys. Rev. A*, **90**, 043828 (2014).
26. Ciurla M., Adamowski J., Szafran B., Bednarek S. *Physica E*, **15**, 261 (2002).
27. Fink J.M., Bianchetti R., Baur M., Göppl M., Steffen L., Filipp S., Leek P.J., Blais A., Wallraff A. *Phys. Rev. Lett.*, **103**, 083601 (2009).
28. Xie Z.G., Solomon G.S. *Appl. Phys. Lett.*, **87**, 093106 (2005).
29. Lovett B.W., Reina J.H., Nazir A., Briggs G.A.D. *Phys. Rev. B*, **68**, 205319 (2003).
30. Nazir A., Lovett B.W., Briggs G.A.D. *Phys. Rev. A*, **70**, 052301 (2004).
31. Golovinskii P.A. *Semicond.*, **48** (6), 760 (2014) [*Fiz. Tekh. Poluprovodn.*, **48**, 781 (2014)]
32. Englund D., Faraon A., Fushman I., Stoltz N., Petroff P., Vučković J. *Nature*, **450**, 857 (2007).